

Using path planning techniques to improve airway tree segmentation from CT images

Paolo Cabras¹ and Jan Rosell¹

¹*Institute of Industrial and Control Engineering, Universitat Politècnica de Catalunya, Barcelona, Spain*
{paolo.cabras,jan.rosell}@upc.edu

Keywords: Airway segmentation : path planning : bronchi connection

Abstract: Virtual Bronchoscopy (VB) permits the preplanning of operations concerning the airways and provides the necessary guidance to reach the pulmonary lesions. Fundamental for a good VB is the reconstruction of a 3D model of the airways from the CT images. Airway segmentation algorithms usually return the biggest detected volume connected to the trachea (the root tree), but many of them also reconstruct during the segmentation process, small parts not connected to the root tree. To overcome this problem this paper proposes a method, based on path planning techniques, that is able to connect the small isolated pieces of bronchi to the terminal points of the root airway tree, taking into account the growing direction of the branches and the gray values of the CT images. As a result, a more complete 3D model of the airways is obtained.

1 INTRODUCTION

Bronchoscopy is an interventional medical procedure used to analyze the tracheobronchial tree, mainly to obtain samples from a specific lung site identified by chest X-ray computed tomography (CT). Virtual Bronchoscopy (VB) is a computer-generated 3D reconstruction that allows physicians to interactively explore the tracheobronchial tree model. VB can make lymph nodes visible by showing the virtual bronchial tubes semitransparent, or can automatically plan a path from the trachea to peripheral lung lesion (Ferguson and McLennan, 2005; Rosell et al., 2012). Recent clinical studies have proved that VB navigation system can effectively shorten the examination and operation time (Shinagawa et al., 2007). Real bronchoscopy aids have also been proposed to guide the execution of the real bronchoscopy using augmented reality techniques, i.e. by superimposing the computed path over the image fed back by the camera, which results in an increase in the success rate to reach the lesion (Eberhardt et al., 2010).

1.1 Motivation

A vital task for the VB is the segmentation of the airway tree from CT slices. This is a difficult task, specially for the the thinnest bronchi, due to image reconstruction artifacts, patient movements or disease

and the partial volume effect. Different segmentation methods have been proposed, that can be divided into three categories (Fetita et al., 2004):

a) 2D/3D techniques: The aim of these techniques is to detect the potential airway regions on 2D axial images and then select the right candidates to reconstruct the 3D model. For instance, (Fetita and Preteux, 1999) use mathematical morphology operations (binary and gray-scale reconstruction) to find the candidates in 2D slices and then the reconstruction of the airway is performed using a 3D propagation driven by 3D topological structure. Usually, the 2D segmentation techniques used may present some difficulties with the smallest bronchi and the obtention of an entirely connected structure may not be possible (if the algorithm fails to detect a candidate bronchus in a single slice then this bronchus is interrupted, preventing the reconstruction from being complete).

b) 3D region growing techniques: Starting with a seed located at the trachea, region growing methods determine the airway region using thresholds (Pinho et al., 2009). The reconstruction accuracy in the region-growing based method depends directly on the threshold settings. Given the great difference in the gray values between biggest and smallest bronchi, a global threshold does not allow to detect and reconstruct a big volume. Better results can be achieved with a dynamic threshold, but also in this case if severe stenosis or local occlusions (due to

noise or pathologies) occur, the growth is blocked and the algorithm fails to detect the distal bronchi due to these interruptions. Consequently, although an algorithm would detect pieces of distal small bronchi, it could happen that these pieces are not considered in the final result since they are not connected to the main tracheobronchial tree.

c) Hybrid methods: Hybrid methods combine the previous approaches. For instance, (Sonka et al., 1996) propose a rule-based method consisting in a combination of 3D seeded region growing to identify large airways, rule-based 2D segmentation of individual CT slices to identify probable locations of smaller diameter airways, and the merging of airway regions across the 3D set of slices. The output is often a non-connected region, i.e. the main tracheobronchial region plus isolated regions segmented as airways but disconnected from it.

To overcome the problem of the isolated segmented regions that appear in any of the above techniques, some algorithms include a final 3D connection step. For instance, in (Bauer et al., 2009b) tubular structures are detected in the data volume and then the different structures are connected together according to branching angle, branch radius and distance. Similarly, (Graham et al., 2010) connects the disjoint branches interpolating their cross sectional surfaces, trying to minimize a connection cost based on the directions of the branches and the gray values of the voxels

Similar disconnection problems appear in digital reconstruction of 3D neuron structures, due to the low single-to-noise ratio of the 3D microscopic images. To solve this problem (Peng et al., 2010) proposed a shortest path graph algorithm that uses both metrics of Euclidean length and of image voxel intensity. In this line, the motivation of the present paper is to contribute to the airway tree segmentation problem with the proposal of a simple yet powerful method based on path planning techniques.

1.2 Path Planning

Path planning is a mature discipline in robotics. The basic path planning problem is focused in the computation of collision free paths for a robot from an initial to a final configuration. This planning is usually done in the robot configuration space (which is a space with dimensionality equal to the degrees of freedom of the robot), where the problem is reduced to the planning of a path of a point (representing the robot) among (accordingly enlarged) obstacles. One of the most used techniques for low dimensional problems is based on the

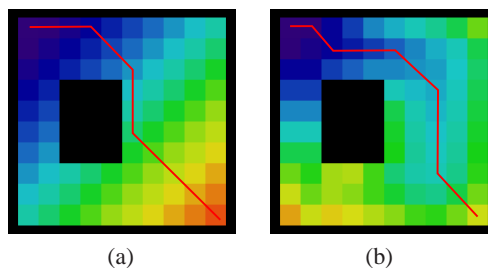


Figure 1: Paths on a 2D space from an initial cell at the bottom-right corner to the goal cell at the top-left one, computed with the NF1 function (a) and with the NF1 function modulated by the clearance (b).

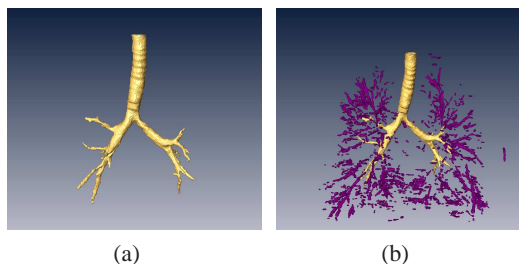


Figure 2: (a) The root tree reconstructed using a region growing method with adaptive threshold; (b) the root tree and the other isolated parts segmented as airways (in purple).

computation of a potential field on a grid representing the discretized configuration space, with a global minima at the goal configuration. The planning is then reduced to the following of the negated gradient of the potential field.

Potential fields can be computed using navigation functions, that are local minima-free potential functions computed over a grid. The navigation function NF1 (Latombe, 1991) is obtained by computing the L1 distances from a cell of the grid (the goal) by a wavefront propagation (Fig. 1a). The problem of the paths obtained with the NF1 navigation function is that they may graze the obstacles, but the potential field provided by a navigation function can be modulated by varying the values being propagated, e.g. by decreasing the potential being propagated by a value proportional to the clearance (Rosell et al., 2012) (Fig. 1b).

1.3 Proposal overview

A stack of CT images of a chest is a 3D grid of voxels with different gray-level values (the darker corresponding to the airways), and the airway segmentation algorithms label these voxels as interior or exterior. All those voxels labeled as interior and connected to the trachea conform the root tree (Fig. 2a). Other isolated sets of voxels labeled

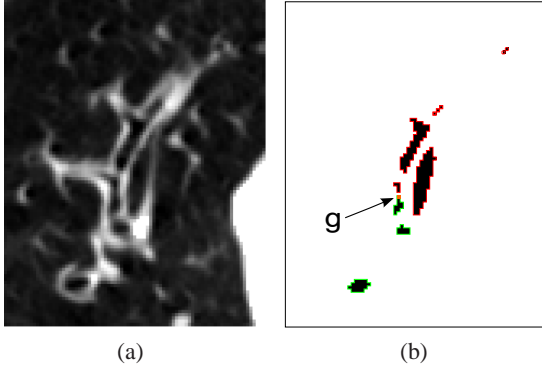


Figure 3: (a) CT slice with a bronchus to be segmented; (b) the result of segmentation: green regions are connected to the root tree, red regions are disconnected. The orange point represent the interruption point g .

as interior but not connected to the root tree may represent parts of interrupted bronchi or badly segmented regions (purple regions in Fig. 2b).

The proposal of the present paper is the use of path planning techniques based on modulations of the navigation function NF1, to connect the set of voxels of an isolated region segmented as airway to the root tree. The proposal is structured in two steps:

1. *Determination of the interrupted branches:* the point where the root tree is interrupted and the direction of the interrupted bronchus are to be determined.
2. *Connection process:* the interrupted branch has to be connected to a candidate isolated region among all the isolated regions around a neighborhood of the interrupted branch point.

Different modulations of the navigation function NF1 will be used in each step.

2 PROPOSED METHOD

This section describes the two steps of the proposal. Although the procedure is done in the 3D grid, for a better comprehension of the whole process, the different steps of the algorithm are illustrated in 2D using the single slice shown in Fig. 3, corresponding to a transversal plane of a stack of CT images. In this figure, a bronchus that evolves horizontally on the slice is shown interrupted: the regions shown in green correspond to regions segmented as airways that are connected to the root tree, the regions shown in red correspond to regions also segmented as airways but disconnected from the root tree (the one on the right is a badly segmented region whereas the other ones correspond to pieces of bronchi).

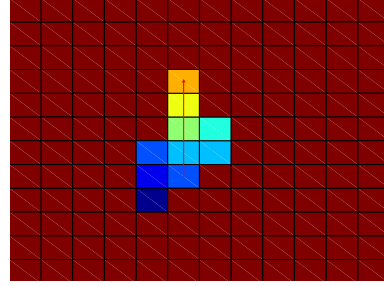


Figure 4: The *regression NF1* function computed on the particular of Fig. 3(b). Warm colors represent highest potential values, cool colors the lowest. Following the negated gradient the origin of the direction vector \mathbf{v}_o is determined.

2.1 Interruption point and direction

The root tree has been computed using a region growing procedure with an adaptive threshold. Then, the points where the root tree is interrupted, i.e. the interruption points, are determined computing the basic NF1 function on the root tree, i.e. propagating a wavefront from the beginning of the trachea and looking for the local maxima of the navigation function. In the 2D example, there is one interruption point, called g , shown in orange in Fig 3b.

The direction of the bronchus at the interruption point is computed using a modulation of the navigation function NF1, called *regressive NF1*. The procedure works as follows:

- A high value is assigned to the interruption point $g = (x_g, y_g, z_g)$ (orange pixel in Fig. 4).
- The potential of each voxel is propagated to its airway neighbors. The value propagated depends on the distance to the walls. Let d_j be the potential of a given voxel j , d_i that of the neighbor voxel i being expanded, c_j be the clearance of node j (i.e. the L1 distance to the non-airway voxels), and C_{max} the maximum clearance. Then:

$$d_j = \begin{cases} d_i - 1 + \frac{C_{max} - c_j}{C_{max}} & \text{if } \frac{C_{max} - c_j}{C_{max}} < 0.9 \\ d_i - 0.1 & \text{otherwise} \end{cases} \quad (1)$$

- Starting at the interruption point, a gradient descent is followed for a given number of steps (currently fixed to five). The reached voxel is labeled as point $o = (x_o, y_o, z_o)$, and the interruption direction is $\mathbf{v}_o = (x_g, y_g, z_g) - (x_o, y_o, z_o)$ (red arrow in Fig. 4).

Fig. 4 is a representation of the *regression NF1* function computed on the example of Fig. 3. This method permits to easily calculate the direction of a branch without knowing the skeleton of the root tree.

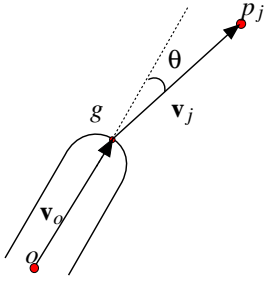


Figure 5: Angle θ between the direction \mathbf{v}_o of the interrupted branch, and the direction \mathbf{v}_j defined by the interruption point g and the current analyzed voxel p_j .

2.2 Connection process

The connection process is done by defining a modulation of the navigation function NF1, called *connection NF1*, on a neighborhood of the interruption point g (this neighborhood is a box centered at g and with 21 voxels per axis). Considering point g as the potential minima, the potential landscape will be modulated to consider:

- The distance to g (the potential of a voxel p_j will be proportional to the L1 distance from g to p_j).
- The directionality (the potential will increase slower in the directions around that defined by the interruption vector \mathbf{v}_o).
- The gray level of the voxels (the potential will increase slower along darker voxels, i.e. those with a higher probability of pertaining to the interior of the airways).

The procedure to compute the *connection NF1* starts assigning a zero value to the interruption point g . Then, the potential is iteratively propagated (within the neighborhood box) as follows:

$$d_j = d_i + (1 - k_G - k_\theta) \quad (2)$$

where:

- k_G depends on the gray level of the considered voxel and on whether the segmentation algorithm has labeled it as airway or not. If S is the set of all the voxels segmented as airways, then:

$$k_G = \begin{cases} 0.98 & \text{if } p_j \in S \\ \min\{0.98, t_{HU} e^{-\frac{1}{2}\left(\frac{t_{HU}-1}{\sigma_{HU}}\right)^2}\} & \text{if } p_j \notin S \end{cases} \quad (3)$$

where t_{HU} is the ratio between the gray level of the voxel and the minimum gray value of the data set¹.

¹HU stands for Hounsfield Units, that is the scale that measures the radiodensity. The darker voxels correspond to the air, that has a value of -1000HU.

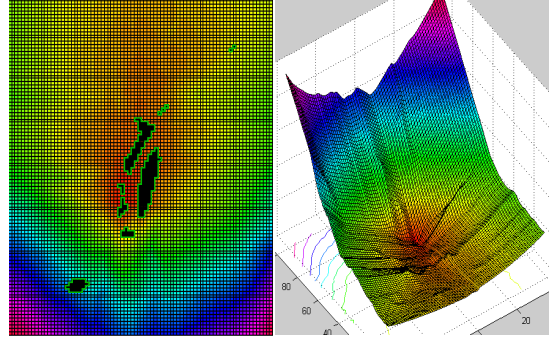


Figure 6: 3D representation of the connection NF1 computed on the 2D scenario of Fig. 3(a).

- k_θ is related to the angle θ between the interruption direction (\mathbf{v}_o) and the vector from point g to the considered voxel p_j , i.e. $\mathbf{v}_j = (x_j, y_j, z_j) - (x_g, y_g, z_g)$ (Fig. 5):

$$k_\theta = \begin{cases} -1 & \text{if } \cos(\theta) < 0 \\ \cos(\theta) e^{-\frac{1}{2}\left(\frac{\theta}{\sigma_\theta}\right)^2} & \text{otherwise} \end{cases} \quad (4)$$

As it can be appreciated, both the gray and orientation terms are modulated by a Gaussian curve which is centered at the minimum gray level of the data set (which correspond to $t_{HU} = 1$) for k_G , and at 0 rad for k_θ . The value of the respective sigmas regulate the width of the “bell curve”. Concerning the direction, (Graham et al., 2010) and (Bauer et al., 2009a) consider that the maximum branching angle for the airway tree is $\pi/3$ rad, and connect only those branches that subtend angles smaller than this value. The proposed modulation of the NF1 function includes such a discrimination, by setting $\sigma_\theta = \pi/6$, i.e. to have a heat attenuation of k_θ in those voxels whose direction is greater than $\pi/3$ rad. On the other hand, all the regions that have a gray value greater than -700 HU are probably not airway lumen voxels, that is why (considering the minimum value equal to -1000 HU) $\sigma = \frac{-700}{-1000} = 0.7$ is set for the Gaussian function of k_G .

Starting at g , the navigation function just defined is computed in all the considered box. With the scenario of Fig. 3 the resulting potential is shown in Fig. 6.

Once the *connection NF1* values are computed, the connection between the root tree and the isolated branches is done with the following steps:

- For each isolated region within the neighbor box, select the point with lowest potential (points e_1 , e_2 and e_3 in Fig. 7a).
- Among the selected points choose the one with lowest potential value (points e_1 in Fig. 7a).

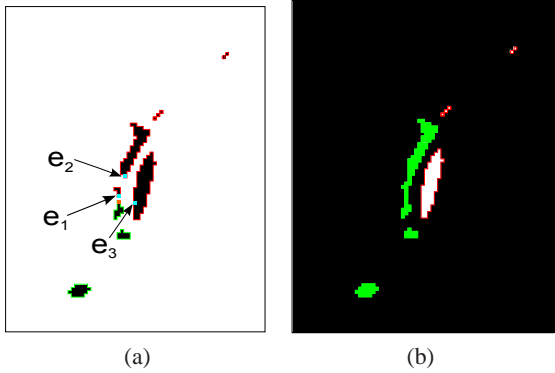


Figure 7: In (a) the interruption point g is shown in orange, the isolated region closest points are shown in cyan. In (b) the connection result is shown (the isolated regions that where bronchi have been correctly connected and the one on the right that was a false positive is not).

- From that point follow the negated gradient of the potential function until the point g with zero potential is reached.
- Label all the voxels of the previous step as airway.

Repeating the whole procedure again, the second isolated region is also connected. It can be appreciated that, thanks to the directionality discriminant, the chosen navigation function avoids the connection with the false positive region on the right labeled as airway lumen by the segmentation algorithm. Fig. 7b shows the final reconstructed bronchus.

3 RESULTS

This section shows some results using the complete 3D stack of CT images that validate the proposed approach. The *regressive NFI* has been able to correctly capture the centerline of the interrupted bronchi without the need to know the entire skeleton of the airway tree; the *connection NFI* function has been able to correctly connect the interrupted point to the correct isolated region, avoiding those false positive regions very near to the interruption point but outside the branch orientation cone or separated from the branch by a vessel or a clear region.

Fig 8 shows an example of the interruption points and of the associated neighborhood boxes where the *connection NFI* is computed to find the connection with the isolated branches that lie within.

Fig. 9 shows in rows two examples of the connection results. The airway tree reconstructed with region growing technique (in gold) and the branches or pieces of branches detected by the

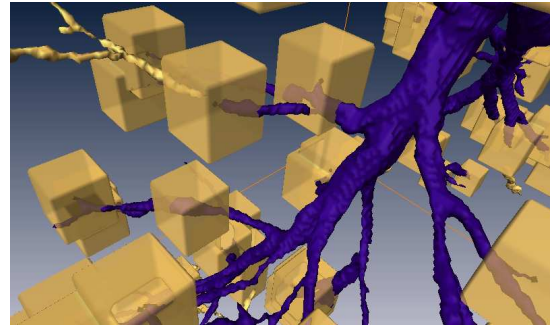


Figure 8: 3D example of the interruption points and the associated neighborhood boxes where the isolated branches to be connected may lie. The root tree is shown in blue, the isolated branches in gold.

segmentation procedure (in purple) are shown on the left; the connection between the root tree and the separated branches is shown in the middle, and the final result is shown on the right.

The current implementation is done using the Amira software and its connection with Matlab. The computational cost is high (it lasts an average of 50 minutes for a whole CT stack) but the qualitative results are very significant since the resulting airway tree can be extended with many already segmented branches that would otherwise be lost.

4 CONCLUSIONS

In the field of airway tree segmentation from CT images, there are many algorithms that return just the root tree even though in previous steps they are able to detect other airway lumen regions which are not present in the final result just because they are not connected to the root tree. With this in mind, this paper has presented a novel approach based on path planning techniques to connect the root tree to those isolated regions that possibly represents a piece of a bronchus. Two local minima-free navigation function have been created to this end, first, to individuate the branch ending direction and, then, to find a path to connect the disconnected branches. The proposal takes as input the result of the segmentation algorithms and return a better airway tree model in terms of completeness, since it can connect the airway root tree to the other isolated detected branches according to the gray level of the regions in the original CT scan and to morphological considerations (orientation and proximity).

Current work includes the implementation of a shape filter to eliminate those disconnected regions that do not appear to be bronchial branches and that

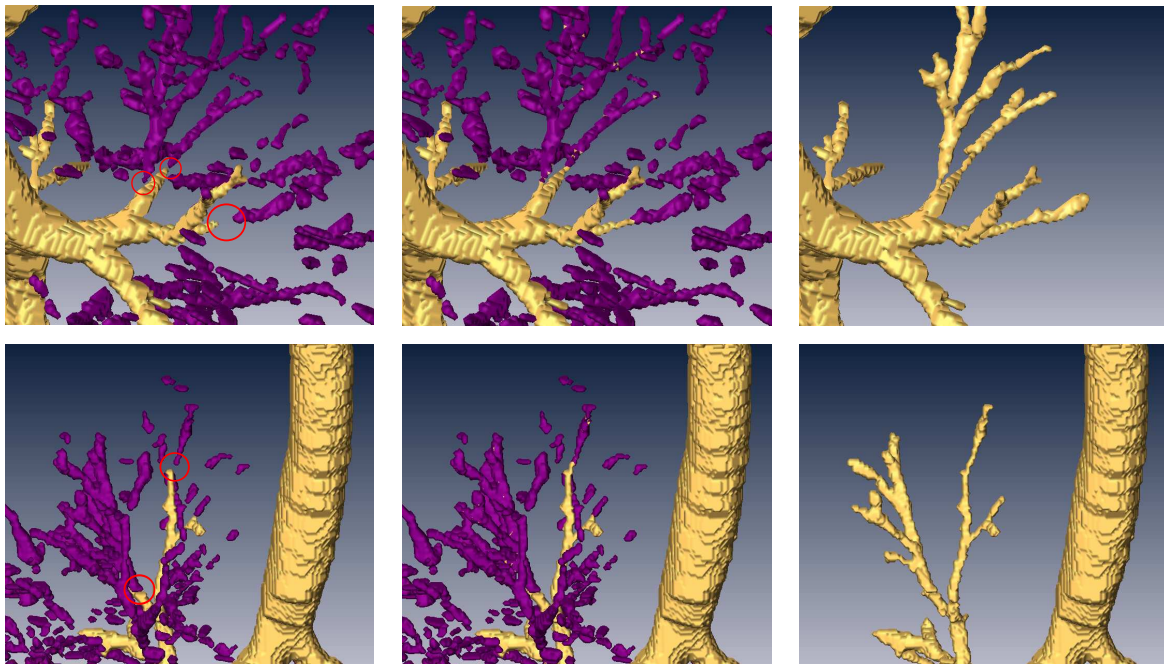


Figure 9: Two examples (in rows) of the 3D connection process. The gold colored region on the left figures is the root tree and the purple volumes are the isolated branches, the parts to be connected are encircled in red. The middle figures show the connection result and the right figures the final airway tree.

are not aligned with the interrupted branch. This will accelerate the computation time of the connection process. Also, a more exhaustive computational evaluation and comparison with other alternatives is under development.

REFERENCES

- Bauer, C., Bischof, H., and Beichel, R. (2009a). Segmentation of airways based on gradient vector flow. In *Second International Workshop on Pulmonary Image Analysis*, pages 191–200. MICCAI.
- Bauer, C., Pock, T., Bischof, H., and Beichel, R. (2009b). Airway tree reconstruction based on tube detection. In *Second International Workshop on Pulmonary Image Analysis*, pages 203–213. MICCAI.
- Eberhardt, R., Kahn, N., Gompelmann, D., Schumann, M., Heussel, C. P., and Herth, F. J. F. (2010). Lungpoint-a new approach to peripheral lesions. *Journal of Thoracic Oncology*, 5(10):1559–1563.
- Ferguson, J. and McLennan, G. (2005). Virtual bronchoscopy. *Proceedings of American Thoracic Society*, 2:488–491.
- Fetita, C. and Prêteux, F. (1999). Three-dimensional reconstruction of human bronchial tree in hrct. In *Proc. of SPIE*, volume 3646, pages 281–294.
- Fetita, C. I., Prêteux, F., Beigelman-Aubry, C., and Grenier, P. (2004). Pulmonary airways: 3-d reconstruction from multislice ct and clinical investigation. *IEEE Transactions on medical imaging*, 23(11):145–152.
- Graham, M. W., Gibbs, J. D., Cornish, D. C., and Higgins, W. E. (2010). Robust 3-d airway tree segmentation for image-guided peripheral bronchoscopy. In *IEEE transactions on Medical Imaging*, volume 29, pages 982–97. IEEE.
- Latombe, J.-C. (1991). *Robot Motion Planning*. Kluwer Academic.
- Peng, H., Ruan, Z., Atasoy, D., and Sternson, S. (2010). Automatic reconstruction of 3d neuron structures using a graph-augmented deformable model. *Bioinformatics*, 26:i38–i46.
- Pinho, R., Luyckx, R., and Sijbers, J. (2009). Robust region growing based intrathoracic airway tree segmentation. *Second International Workshop on Pulmonary Image Analysis*, pages 261–277.
- Rosell, J., Perez, A., Cabras, P., and Rosell, A. (2012). Motion planning for the virtual bronchoscopy. In *IEEE International Conference on Robotics and Automation*, pages 2932 – 2937. IEEE.
- Shinagawa, N., Yamazaki, K., Onodera, Y., Asano, F., Ishida, T., Moriya, H., and Nishimura, M. (2007). Virtual bronchoscopy navigation system shortens the examination time: Feasibility study of virtual bronchoscopy navigation system. *Lung Cancer*, 56(2):201–206.
- Sonka, M., Park, W., and Hoffman, E. A. (1996). Rule-based detection of intrathoracic airway trees. In *IEEE transactions on Medical Imaging*, volume 15, pages 314–326. IEEE.